Applied Chemical Engineering (2019) Volume 2 Issue 1
doi:10.24294/ace.v2i1.641

Effect of Zn^{2+} Concentration on the Zinc Oxide Properties Prepared by Electrochemical Deposition

A. Henni[1,2*], A. Karar[3], A. Merrouche[1], L. Telli[1]

[1] Laboratoire des Matériaux inorganiques, Université Mohamed Boudiaf - M'Sila, 28000, Algeria. E-mail: henni.abdellah@gmail.com

[2] Kasdi Merbeh University, Ouargla 30000, Algeria.

[3] Laboratoire d'Energétique et d'Electrochimie du solide, Université Ferhat Abbas-Sétif 1, 19000 Algeria.

ABSTRACT

In this work, ZnO nanostructures are electrodeposited on ITO conducting substrate prepared from chloride baths. The influence of concentration of Zn^{2+} on the electrochemical characteristics has been studied using cyclic voltammetry (CV) and chronoamperometry (CA) techniques. The Mott–Schottky measurements demonstrate an n-type semiconductor character for all samples with a carrier density varying between 1.47 × 1,018 cm^{-3} and 3.14 × 1,018 cm^{-3}. Scanning electron microscopy (SEM) show arrays of vertically aligned ZnO nanorods (NRs) with good homogeneity. X-ray diffraction spectra demonstrate that films crystalline with the Würtzite structure with preferential (002) crystallographic orientation having c-axis perpendicular to the substrate. The high optical properties of the ZnO NRs with a low density of deep defects was checked by UV-Vis transmittance analyses, the band gap energy of films varies between 3.3 and 3.4 eV with transparency around 80-90%.

Keywords: Electrochemical Growth; Zno; Nanorods; Thin Films; Zinc Concentration

1. Introduction

Zinc oxide (ZnO) presents an optical band gap close to 3.37 eV[1] at room temperature, high transparency[2], excellent thermal stability[3], pyroelectric[4] and piezoelectric[5] properties. Aside from its interesting characteristics, it has a relatively low cost and low toxicity[3-7]. For these reasons, ZnO is considered as a good candidate for optical devices in the near UV region[8], and for the short wavelength-emitting devices such as light emitting diodes[2]. ZnO with different morphologies can be prepared by various deposition techniques such as magnetron sputtering[9], chemical vapour deposition[10], pulsed laser deposition[11], spray pyrolysis[12] or thermal evaporation[13] and so on. Among all approaches, electrodeposition technique has been emerging as a competitive technique for the fabrication of metallic oxide semiconductor nanostructures with different shape and sizes[14-17].

Electrodeposition method has several advantages[18,19] compared to other techniques: easy control of the thickness and the morphology of the film, simplicity, low equipment cost and possibility of making large-area thin films. For the electrodeposition of ZnO, the majority of the published works used nitrate ions[17,20] or molecular oxygen[21,22] as precursors. However, few studies have been presented using hydrogen peroxide as a precursor[23]. The aim of this work is to investigate the influence of $ZnCl_2$ concentration on the electrodeposition process, optical and electrochemical properties of the oriented ZnO nanorods.

2. Experimental

Zinc oxide nanostructures were prepared by electrochemical deposition onto indium doped tin oxide

doi: 10.24294/ace.v2i1.641

(ITO, 25Ω/sq) glass coated substrates. The ITO substrates were ultrasound cleaned sequentially with acetone, ethanol and distilled water. After the ultrasound cleaning process, the ITO glass was finally rinsed with distilled water and dried in air. The electrochemical deposition of ZnO was carried out in a three-electrode cell that consists a platinum electrode as counter-electrode, a saturated calomel electrode as reference (SCE). The electrodeposition of ZnO nanostructures and cyclic voltammetry (CV) measurements were carried out using, a computer-controlled potentiostat/galvanostat (Autolab PGSTAT 302N) using the NOVA software. The initial solution is composed of 0.1 M KCl, 5 mM H_2O_2[14], and $ZnCl_2$ with various concentrations (2, 5, 7 and 10 mM). Electrodeposition was performed at about 70 °C in a potentiostatic mode at -1.0V vs. SCE for 40 min.

The ZnO film/electrolyte capacitance measurements were performed in the same electrochemical cell with the same device as used for ZnO electrodeposition. Surface morphology was studied by scanning electron microscopy (SEM) with JEOL JSM-7001F. Phases and crystal structures were characterized by X-ray diffraction (XRD) with a Bruker AXS D8 Advance with a Cu $K\alpha_1$ radiation (1.5406 Å). The UV-Vis transmittance spectra were recorded with a Shimadzu UV-1800 spectrophotometer.

3. Results and discussion

Figure 1 shows the cyclic voltammetric scans performed in 5 mM of H_2O_2 and 0.1 M of KCl and a variable $ZnCl_2$ concentration. The cyclic voltammetric measurements are performed to identify the oxidation-reduction processes potentially undergone by the system. During forward scan, a cathodic current observed relating to the following reaction[24]:

$$H_2O_2 + 2e^- \rightarrow 2OH^- \quad (1)$$

Then, the zinc ions react with the hydroxide groups on the substrate surface to form the zinc hydroxide. At 70 °C, $Zn(OH)_2$ dehydrates spontaneously following:

$$Zn^{2+} + 2OH^- \rightarrow Zn(OH)_2 \quad (2)$$

$$Zn(OH)_2 \rightarrow ZnO + H_2O \quad (3)$$

It also shows an increase of the current density of reduction with the concentration of $ZnCl_2$. The ZnO can be electrodeposited in the range leading to the H_2O_2 reduction process. The voltammograms shows no phenomenon other than the reduction of H_2O_2.

Morphology of the obtained films at different Zn^{2+} concentrations is presented in inset of **Figure 1**. Homogeneous ZnO nanorods have been obtained over the entire ITO substrate, which is very interesting for the realization of dye-sensitized solar cell (DSSC)[25,26]. The nanorods act as a direct pathway for the electron transfer from the excited dye to the front contact, which favours the charge collection in the cell. The nanorods of ZnO films are hexagonal in shape with a smooth top surface, that a diameter varying in the range 115-185 nm. The crystallites present both a lateral and a vertical growth. If the hydroxides ions generated at the electrode surface are in excess in the solution, the zinc ions present in the vicinity of the electrode are consumed rapidly and the local pH increases progressively. In first time the crystallites grow in the lateral and the vertical directions. Then, the lateral growth is then completely quenched. However, the rod growth is not fully stopped and the crystallites continue to growth but only in the c-direction.

Figure 2 shows the X-ray diffraction spectra of ZnO nanostructured films grown at different H_2O_2 concentrations. The films exhibit good crystallinity and all the peaks are indexed to the Würtzite hexagonal ZnO lattice (JCPDS no. 36-1451). The peaks marked with an asterisk (*) are assigned to ITO substrates, and no additional peaks corresponding to Zn or other impurities were present. The XRD patterns for all samples of ZnO show only one intense diffraction peak that located at ~34.44° which can be attributed to (002) plan,

suggesting that ZnO crystallites are highly oriented with the c-axis being perpendicular to the substrate.

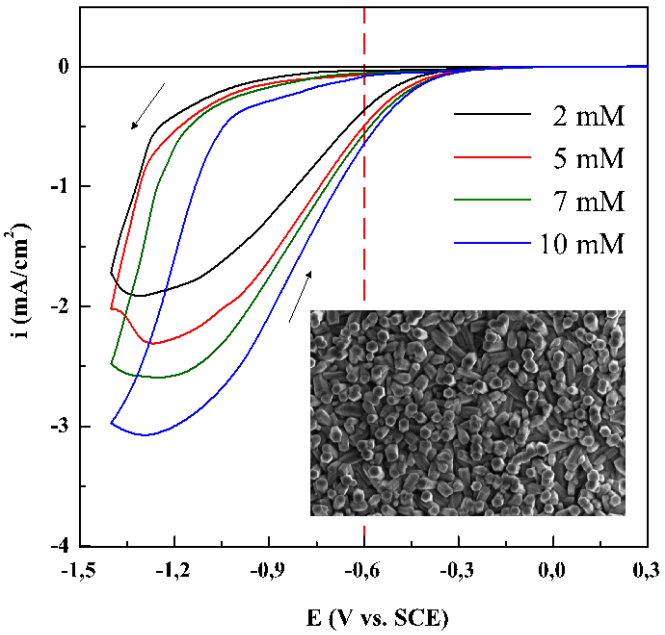

Figure 1. Voltammograms on ITO substrate from aqueous solution containing 5 mM H_2O_2 and 0.1 M KCl at various $ZnCl_2$ concentrations. T = 70 °C and potential scan rate is 10 mV/s. Inset: The morphology obtained films.

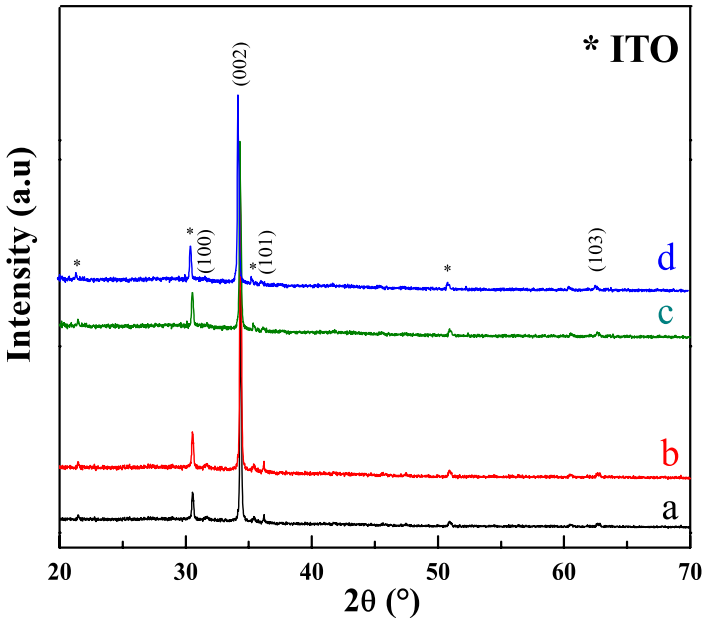

Figure 2. XRD patterns of films deposited at different $ZnCl_2$ concentrations: (a) 2, (b) 5, (c) 7 and (d) 10 mM. * Fo ITO diffraction peaks.

Mott–Schottky measurements were used to determine both doping density and flat band potential at semiconductor/liquid contacts. Mott–Schottky plot of the space charge capacitance is presented for ZnO layers obtained at different $ZnCl_2$ concentrations according to the following relationship[27]:

$$\frac{1}{C_{SC}^2} = \left(\frac{2}{qA^2 N_D \varepsilon \varepsilon_0}\right)\left(E - E_{fb} - \frac{kT}{q}\right) \quad (4)$$

In this equation, C_{SC} represents the space charge capacitance, ε is the dielectric constant of ZnO, ε_0 is the permittivity of free space, N_D is the carrier concentration, E_{fb} is the flat band potential, k is Boltz-

mann's constant, T is the absolute temperature and q is the elementary electron charge.

According to the Mott–Schottky plot (**Figure 3**), a linear relationship of C_{SC}^{-2} vs. E was observed. The potential at which the line intersects the potential axis gives the flat band potential (E_{fb}) and the slope yields the carrier concentration (N_D) of the sample. The positive slopes of the straight lines indicate the n-type conductivity of the ZnO thin films. Thus from **Figure 3**, a $E_{fb} = 0.12 \pm 0.04$ V was obtained for all samples. The carrier density fluctuates from 1.47×10^{18} to 3.14×10^{18} and the increase with $ZnCl_2$ concentration. These values are typically those of no doping nanostructured ZnO[28].

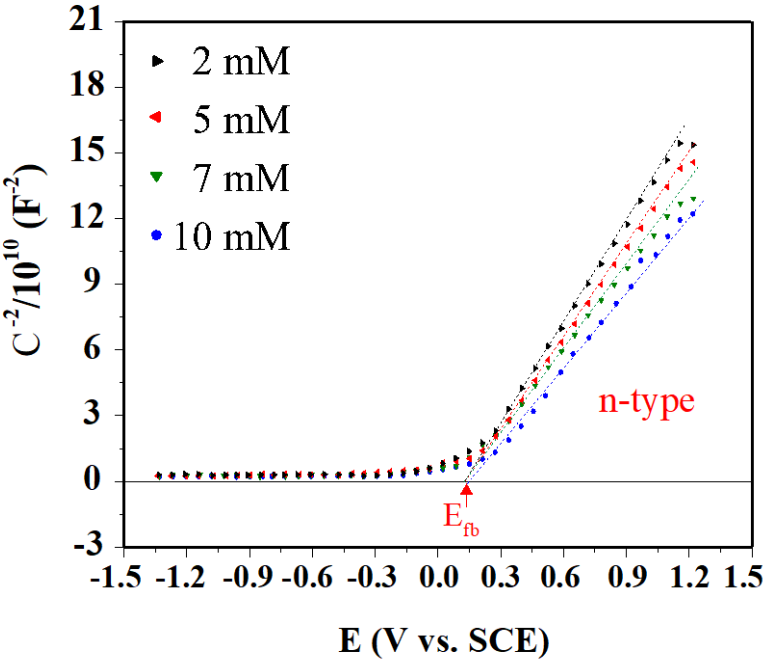

Figure 3. Mott-Schottky plots of the ZnO layers deposited at different $ZnCl_2$ concentrations recorded at 0.2 kHz.

The optical transmission spectra recorded in the range of 300 to 750 nm of the ZnO nanostructures deposited at different concentrations of $ZnCl_2$ are shown in **Figure 4**. We observe that the transmittance is high, around 80-100% with increasing $ZnCl_2$ concentrations. The energy band gap (E_g) for ZnO was evaluated by using the Tauc plot[29]. The values of the energy band gap of ZnO layers (**Figure 5**) are determined from the intercept of the straight-line portion at the horizontal axis when $\alpha h\upsilon = 0$, these values of E_g vary between 3.3 and 3.4 eV. The optical band gap decreases with increasing the concentration of $ZnCl_2$.

4. Conclusion

ZnO nanorods array films with good transparency, and homogeneity were successfully electrodeposited onto ITO coated glass substrates using an aqueous chloride zinc solution and H_2O_2 as OH^- precursors. The optimal $ZnCl_2$ concentration for the growth of ZnO nanorods was established. XRD characterizations show that the films are crystallized in the Würtzite hexagonal structure with a very high crystallite orientation along the c-axis; a (002) orientation was obtained for the 5 mM concentration of $ZnCl_2$. The SEM micrographs confirms this result, where nanorods hexagonal shapes perpendicular to the substrate surface were obtained under these conditions. The Mott-Schottky plot shows that the films are n-type semiconductors. A high apparent donor density was calculated for samples elaborated. The band gap energy values of the obtained ZnO were found to change between 3.3 and 3.4 eV when the $ZnCl_2$ concentration varied between 2 and 10 mM.

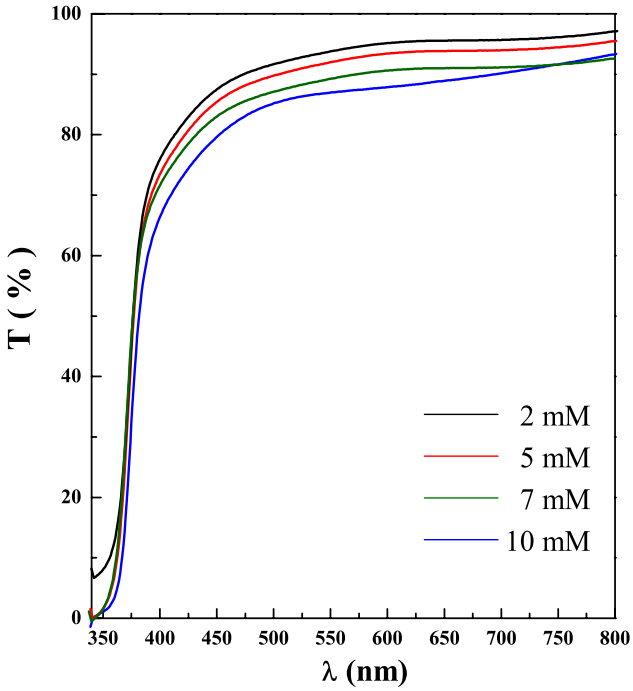

Figure 4. Transmittance spectra of a ZnO layers on ITO-coated conducting glass surfaces obtained at different H_2O_2 concentrations.

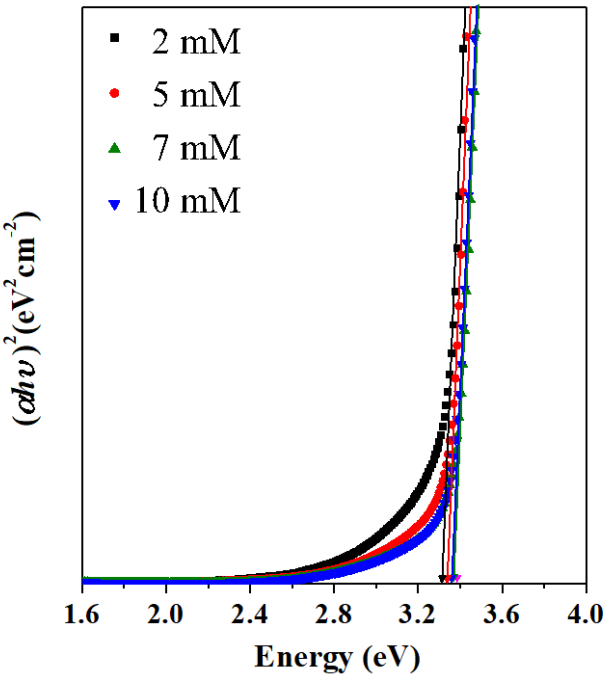

Figure 5. $(\alpha h\upsilon)^2$ vs. energy dependence for the determination of the optical band gap energy.

Conflict of interest

The authors declared no conflict of interest.

References

1. Sepulveda-Guzman S, Reeja-Jayan B, de la Rosa E, *et al*. Synthesis of assembled ZnO structures by precipitation method in aqueous media. Materials Chemistry and Physics 2009; 115(1): 172–178.
2. Lupan O, Guérin VM, Tiginyanu IM, *et al.* Well-aligned arrays of vertically oriented ZnO nanowires electrodepos-

ited on ITO-coated glass and their integration in dye sensitized solar cells. Journal of Photochemistry and Photobiology A: Chemistry 2010; 211(1): 65–73.
3. O'Brien S, Nolan MG, Çopuroglu M, *et al.* Zinc oxide thin films: Characterization and potential applications. Thin Solid Films 2010; 518(16): 4515–4519.
4. Yang Y, Guo W, Pradel KC, *et al.* Pyroelectric nanogenerators for harvesting thermoelectric energy. Nano Letters 2012; 12(6): 2833–2838.
5. Pradhan D, Leung KT. Controlled growth of two-dimensional and one-dimensional ZnO nanostructures on indium tin oxide coated glass by direct electrodeposition. Langmuir 2008; 24(17): 9707–9716.
6. Chu D, Hamada T, Kato K, *et al.* Growth and electrical properties of ZnO films prepared by chemical bath deposition method. Physica Status Solidi (a) 2009; 206(4): 718–723.
7. Chang YN, Zhang M, Xia L, *et al.* The toxic effects and mechanisms of CuO and ZnO nanoparticles. Materials 2012; 5(12): 2850–2871.
8. Luo L, Zhang Y, Mao SS, *et al.* Fabrication and characterization of ZnO nanowires based UV photodiodes. Sensors and Actuators A: Physical 2006; 127(2): 201–206.
9. Minami T, Yamamoto T, Miyata T. Highly transparent and conductive rare earth-doped ZnO thin films prepared by magnetron sputtering. Thin Solid Films 2000; 366(1–2): 63–68.
10. Ateav BM, Bagamadova AM, Mamedov VV, *et al.* Thermally stable, highly conductive, and transparent ZnO layers prepared in situ by chemical vapor deposition. Materials Science and Engineering: B 1999; 65(3): 159–163.
11. Sun XW, Kwok HSK. Optical properties of epitaxially grown zinc oxide films on sapphire by pulsed laser deposition. Journal of Applied Physics 1999; 86(1): 408–411.
12. El Hichou A, Addou M, Ebothé J, *et al.* Influence of deposition temperature (Ts), air flow rate (f) and precursors on cathodoluminescence properties of ZnO thin films prepared by spray pyrolysis. Journal of luminescence 2005; 113(3–4): 183–190.
13. Srivatsa KMK, Chhikara D, Kumar MS. Synthesis of aligned ZnO nanorod array on silicon and sapphire substrates by thermal evaporation technique. Journal of Materials Science & Technology 2011; 27(8): 701–706.
14. Henni A, Merrouche A, Telli L, *et al.* Effect of H_2O_2 concentration on electrochemical growth and properties of vertically oriented ZnO nanorods electrodeposited from chloride solutions. Materials Science in Semiconductor Processing 2015; 40: 585–590.
15. Henni A, Merrouche A, Telli L, *et al.* Optical, structural, and photoelectrochemical properties of nanostructured ln-doped ZnO via electrodepositing method. Journal of Solid State Electrochemistry 2016; 20(8): 2135–2142.
16. Henni A, Merrouche A, Telli L, *et al.* Studies on the structural, morphological, optical and electrical properties of Al-doped ZnO nanorods prepared by electrochemical deposition. Journal of Electroanalytical Chemistry 2016; 763: 149–154.
17. Khelladi MR, Mentar L, Beniaiche A, *et al.* A study on electrodeposited zinc oxide nanostructures. Journal of Materials Science: Materials in Electronics 2013; 24(1): 153–159.
18. Izaki M, Omi T. Transparent zinc oxide films prepared by electrochemical reaction. Applied Physics Letters 1996; 68(17): 2439–2440.
19. Goux A, Pauporte T, Chivot J, *et al.* Temperature effects on ZnO electrodeposition. Electrochimica Acta 2005; 50(11): 2239–2248
20. Singh T, Pandya DK, Singh R. Effect of supporting electrolytes on the growth and optical properties of electrochemically deposited ZnO nanorods. Optical Materials 2013; 35(7): 1493–1497.
21. Izaki M, Omi T. Electrolyte optimization for cathodic growth of zinc oxide films. Journal of the Electrochemical Society 1996; 143(3): L53.
22. Gu ZH, Fahidy TZ. Electrochemical deposition of ZnO thin films on Tin-Coated glasses. Journal of the Electrochemical Society 1999; 146(1): 156.
23. Ramirez D, Silva D, Gomez H, *et al.* Electrodeposition of ZnO thin films by using molecular oxygen and hydrogen peroxide as oxygen precursors: Structural and optical properties. Solar Energy Materials and Solar Cells 2007; 91(15–16): 1458–1461.
24. Pauporte T, Lincot D. Hydrogen peroxide oxygen precursor for zinc oxide electrodeposition II—Mechanistic aspects. Journal of Electroanalytical Chemistry 2001; 517(1–2): 54–62.
25. Qi L, Yu H, Lei Z, *et al.* Dye-sensitized solar cells based on ZnO nanowire array/TiO_2 nanoparticle composite photoelectrodes with controllable nanowire aspect ratio. Applied Physics A 2013; 111(1): 279–284.
26. Kao MC, Chen HZ, Young SL. Effects of preannealing temperature of ZnO thin films on the performance of dye-sensitized solar cells. Applied Physics A 2010; 98(3): 595–599.
27. Morrison SR. Electrochemistry at semiconductor and oxidized metal electrodes. New York: Plenum Press; 1980. p. 127.
28. Pradhan D, Mohapatra SK, Tymen S, *et al.* Morphology-controlled ZnO nanomaterials for enhanced photoelectrochemical performance. Materials Express 2011; 1(1): 59–67.
29. Tauc J, Grigorovici R, Vancu A. Optical properties and electronic structure of amorphous germanium. Physica Status Solidi (b) 1966; 15(2): 627–637.